

## Laser and Fourier Transform Spectroscopy of the [23.8]1–X 0<sup>+</sup> System of ReN

R. S. RAM,\*† P. F. BERNATH,\*† W. J. BALFOUR,‡ J. CAO,‡  
C. X. W. QIAN,‡ AND S. J. RIXON‡<sup>1</sup>

\**Department of Chemistry, University of Arizona, Tucson, Arizona 85721; †Department of Chemistry, University of Waterloo, Waterloo, Ontario, Canada N2L 3G1; and ‡Department of Chemistry, University of Victoria, Victoria, British Columbia, Canada V8W 3P6*

The emission spectrum of ReN has been observed in the 400–476 nm spectral region using a Fourier transform spectrometer. The bands were excited in a rhenium hollow cathode lamp in the presence of a trace of N<sub>2</sub>. The observed bands, with the 0–0 band at 23 746.42 cm<sup>-1</sup>, have been assigned as the [23.8]1–X 0<sup>+</sup> electronic transition. A rotational analysis of the 0–1, 0–0, and 1–0 bands for both <sup>187</sup>ReN and <sup>185</sup>ReN isotopomers has been performed. The principal ground state equilibrium molecular constants for <sup>187</sup>ReN obtained from this analysis are  $B_e'' = 0.482414(11)$  cm<sup>-1</sup>,  $r_e'' = 1.63780(2)$  Å, while the corresponding excited state values are  $B_e' = 0.441093(13)$  cm<sup>-1</sup>,  $r_e' = 1.71280(3)$  Å. The 0–0 band was also observed by pulsed dye laser excitation spectroscopy using a free jet expansion source. In this experiment, the ReN was made by laser vaporization of a rhenium rod followed by reaction with NH<sub>3</sub>. The excited [23.8]1 state has a fluorescence lifetime of 201 ± 1 nsec. There are no previously reported observations of the ReN molecule. © 1994 Academic Press, Inc.

### INTRODUCTION

The diatomic transition metal nitrides provide the simplest models for the bonding of nitrogen atoms to transition metals. Such studies are important in the study of catalytic processes involving the transition metal elements (1). The solid transition metal nitrides are hard refractory materials that are formed at high temperatures by the reaction of metals with N<sub>2</sub> or NH<sub>3</sub> (2). Although the optical spectra of many gaseous transition metal oxides and hydrides are relatively well characterized, only a few nitrides are known. Since the first observation of the gas-phase spectra of MoN (3) and NbN (4) in 1960s, several gaseous transition metal nitrides have been characterized experimentally. The other diatomic transition metal nitrides for which gas-phase data are available include ScN (5), WN (6), YN (7), TiN (8, 9), VN (10–12), and ZrN (13). The matrix isolation studies of some of transition metal nitrides are also available, for example, for TaN (14), ZrN (15), MoN (16, 17), and NbN (18). Mass spectrometric data for several transition metal nitrides by Gingerich (19) indicate that the early transition metal nitrides have significant bond energies ranging from 400 to 600 kJ/mole.

There is no previous experimental or theoretical work on ReN. In fact, among rhenium-containing diatomic molecules only ReO (20, 21) and ReF (22) have been characterized spectroscopically. Recently, two of the authors have observed the Fourier transform emission spectra of several new diatomic nitrides such as ScN (5), WN

<sup>1</sup> Also with the Department of Physics and Astronomy, University of Victoria, Victoria, B.C., Canada V8W 3P6.

(6), and YN (7). Continuing this project, we report the discovery of another gas-phase transition metal nitride, ReN.

At almost the same time as the Fourier transform experiments were carried out at Kitt Peak, the spectrum of ReN was also observed in Victoria by laser excitation spectroscopy of a cold free jet expansion. In this case, the ReN was made by pulsed laser ablation of a Re rod and subsequent reaction of the metal vapor with  $\text{NH}_3$ . Since these experiments involve the absorption of laser light by cold molecules, they complement the Fourier transform emission spectra.

Like many transition metal oxides, diatomic transition metal nitrides are expected to produce complex spectra due to the high spin coupling of the  $d$  electrons resulting in electronic states with high multiplicity. The situation becomes worse for the heavy  $5d$  transition metal oxides and nitrides because strong spin-orbit interactions limit the validity of the  $S$ ,  $\Sigma$ , and  $\Lambda$  quantum numbers. The different spin components of a  $^{2S+1}\Lambda$  term are split into widely separated  $\Omega$  states with Hund's case ( $c$ ) type of electronic structure. This makes the definite characterization of the electronic states in these molecules more difficult. The observed ReN bands involve a  $\Delta\Omega = 1$  transition with the lower state a Hund's case ( $c$ )  $X0^+$  ground state.

#### EXPERIMENTAL DETAILS

##### (a) *Fourier Transform Emission Spectroscopy*

The spectrum of the ReN molecule was observed with a rhenium hollow cathode lamp. The cathode was prepared by inserting a 0.5-mm-thick cylindrical foil of rhenium metal into a hole in a copper block. The foil was tightly pressed against the inner wall of the hole to provide a close and uniform contact between the metal and the copper. The lamp was operated at 300 V and 457 mA current with a slow continuous flow of about 3 Torr of neon and about 5 mTorr of  $\text{N}_2$ .

The spectra were recorded using the 1-m Fourier transform spectrometer associated with the McMath Solar Telescope of the National Solar Observatory. The spectra in the 10 000–29 000  $\text{cm}^{-1}$  region were recorded in two experiments. The 10 000–19 500  $\text{cm}^{-1}$  region was recorded using Si-diode detectors and 495-nm red-pass filters (RG495) and six scans were coadded in 1 h of integration. For the 17 000–29 000  $\text{cm}^{-1}$  spectral region, the spectrometer was operated with  $\text{CuSO}_4$  filters and Si-diode detectors. This time a total of eight scans were coadded in approximately 1 h of integration. In both cases the spectrometer resolution was set at 0.02  $\text{cm}^{-1}$  and the observed interferograms were transformed on the mountain to provide the spectra of ReN.

In addition to ReN bands, the final spectra contained several bands belonging to  $\text{N}_2$  and  $\text{N}_2^+$  as well as Re and Ne atomic lines. The spectra were calibrated using the measurements of the Ne atomic lines made by Palmer and Engleman (23). Some of the ReN transitions are overlapped by strong  $\text{N}_2^+$  transitions and could not be measured reliably. The absolute accuracy of the wavenumber scale is expected to be better than  $\pm 0.002 \text{ cm}^{-1}$ . The ReN lines have a width of 0.065  $\text{cm}^{-1}$  and appear with a maximum signal-to-noise ratio of 10:1 limiting the precision of measurements of strong and unblended ReN lines to  $\pm 0.003 \text{ cm}^{-1}$ .

##### (b) *Laser Excitation Spectroscopy*

ReN was generated with a laser ablation source at the University of Victoria. The source consists of a pulsed supersonic molecular beam with a rotating metal rod attached near the orifice of the nozzle (24, 25). A rhenium rod (5 mm diameter, Johnson

Matthey, 99.99%) and an  $\text{NH}_3/\text{He}$  (20/740 Torr) mixture were used in the experiment. The second harmonic of a Nd:YAG laser (Continuum NY61) was used as the ablation source with a typical pulse energy of 300 mJ. The laser induced fluorescence spectrum was then recorded using a pulsed dye laser pumped by a second Nd:YAG laser (Lumonics YM600, HD500). The linewidth of the dye laser is  $0.1 \text{ cm}^{-1}$ . The emission following the dye laser excitation was detected with a monochromator/PMT assembly. A fluorescence decay curve of the excited state was also recorded at the bandhead of the 0–0 band.

## RESULTS

### (a) Fourier Transform Spectroscopy

The spectral line positions were extracted from the observed spectra using a data reduction program called PC-DECOMP developed by J. Brault of the National Solar Observatory at Kitt Peak. The peak positions were determined by fitting a Voigt line-shape function to each spectral feature. The line positions and intensities were used as input to PC-LOOMIS, an interactive color Loomis–Wood program developed at Arizona by C.N. Jarman. PC-LOOMIS is of great assistance in rapidly picking out branches of weak bands in complex spectra.

Several ReN bands have been observed in the  $21\,000\text{--}25\,000 \text{ cm}^{-1}$  spectral region. In this region, there are three prominent bands with *R* heads at  $22\,624$ ,  $23\,751$  and  $24\,622 \text{ cm}^{-1}$ . The wavenumber separation and the relative intensity of these bands together with the sign and magnitude of the  $^{185}\text{Re}/^{187}\text{Re}$  isotopic shifts indicates that these bands are the 0–1, 0–0, and the 1–0 bands of a single electronic transition. The Re atom has two naturally occurring isotopes,  $^{187}\text{Re}$  and  $^{185}\text{Re}$ , with abundances of 62.93 and 37.07%, respectively. The isotopic splitting is well resolved in the 0–1 and the 1–0 bands. The vibrational assignment was subsequently confirmed by detailed rotational analysis of both isotopomers of ReN.

In addition to these bands, there are several very weak bands near  $22\,230$  and  $25\,495 \text{ cm}^{-1}$  which remain unassigned and improved spectra are required for definite characterization. These bands do not seem to belong to the transition discussed in detail in this paper.

A part of the spectrum of the 0–0 band is shown in Fig. 1. The structure of this band consists of three branches, *P*, *Q*, and *R*, consistent with a  $\Delta\Omega = \pm 1$  transition. The intensity of the *R* branch is greater than that of the *P* branch, and the *Q* branch is the strongest branch. On this basis we concluded that this transition most probably involves a  $\Delta\Omega = +1$  transition. In the 0–0 band, the  $^{185}\text{Re}/^{187}\text{Re}$  isotopic splitting is not resolved for the lower *J* values. At higher *J*, the lines become broad and are split into two components with a 3:1 intensity ratio consistent with  $^{185}\text{Re}/^{187}\text{Re}$  isotopic abundances. The isotopic splittings are particularly noticeable in the *Q* and *P* branches.

A part of the 1–0 band showing the isotopic splitting is presented in Fig. 2. We have measured the rotational structure of both isotopomers in order to determine independent molecular constants for  $^{185}\text{ReN}$  and  $^{187}\text{ReN}$ . The transition wavenumbers for  $^{185}\text{ReN}$  and  $^{187}\text{ReN}$  are presented in Tables I and II, respectively. No rotational perturbations have been observed in any of the analyzed bands. The molecular constants were determined by fitting the observed transition wavenumbers to the rotational energy level expression:

$$F_v(J) = T_v + B_v J(J+1) - D_v [J(J+1)]^2 + H_v [J(J+1)]^3 \\ \pm \delta_{a,1}/2 \{ q(J(J+1) + q_D [J(J+1)]^2 + q_H [J(J+1)]^3 \}.$$

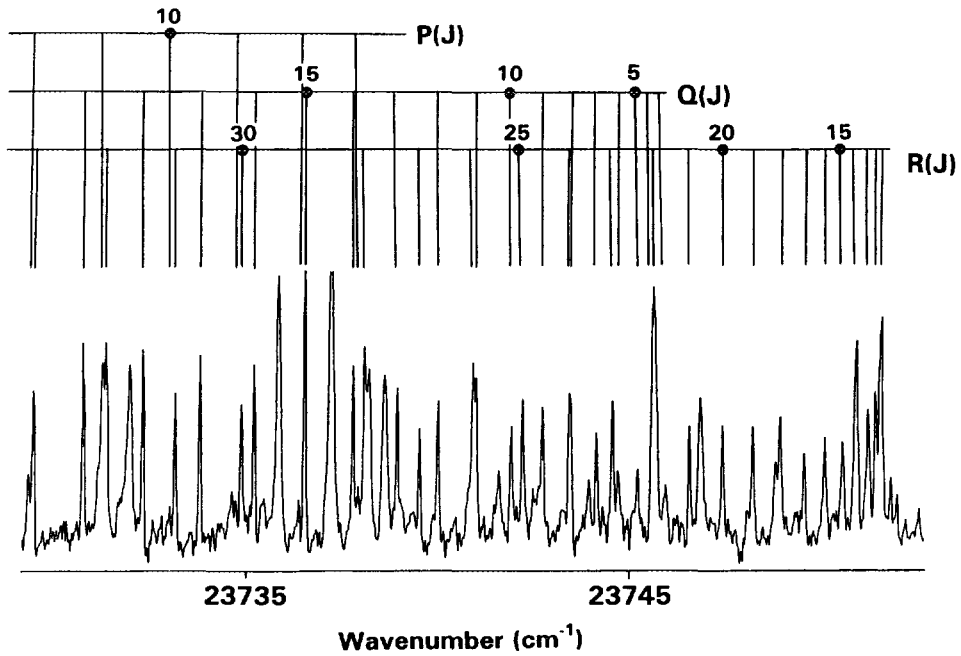


FIG. 1. A part of the 0-0 band of the [23.8]1-X0<sup>+</sup> system of ReN near the bandhead.

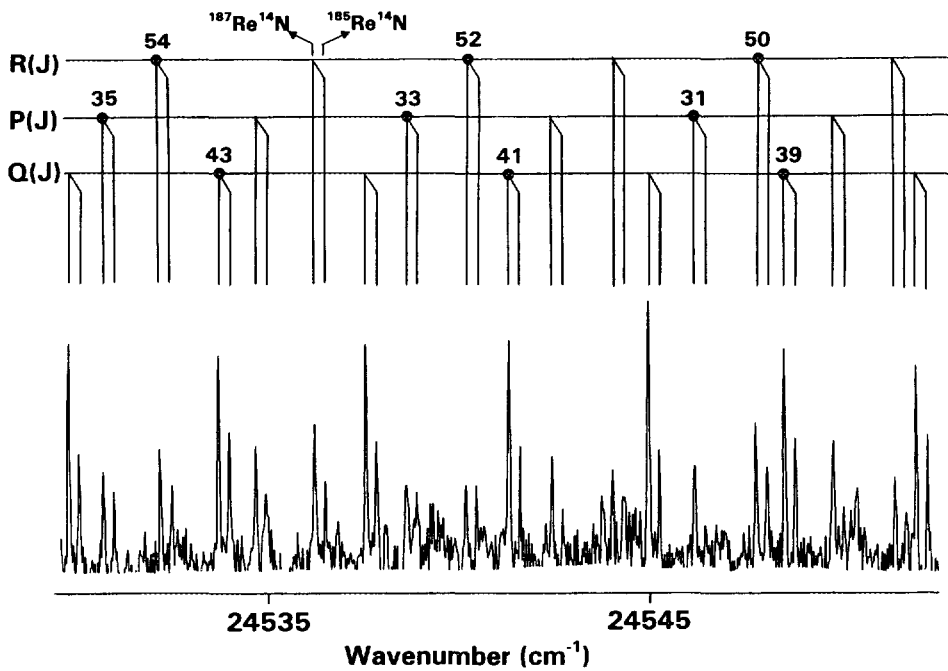


FIG. 2. A part of the 1-0 band of the [23.8]1-X0<sup>+</sup> system of ReN showing <sup>185</sup>ReN/<sup>187</sup>ReN isotope shifts.

TABLE I

Observed Wavenumbers (in  $\text{cm}^{-1}$ ) of the 0-1, 0-0, and 1-0 Bands of the  $[23.8]1-X^0+$  System of  $^{185}\text{ReN}$ 

0-1 BAND						0-0 BAND						1-0 BAND						
J	R(J)	O-C	Q(J)	O-C <sup>a</sup>	P(J)	O-C	R(J)	O-C	Q(J)	O-C	P(J)	O-C	R(J)	O-C	Q(J)	O-C	P(J)	O-C
3									23745.926		3							
4									23745.590		-4							
5									23745.185		1							
6							23750.816	-9	23744.687		-3							
7							23751.116	-7	23744.125	10	23737.921	-13						
8	22629.602	3	22621.724	4			23751.357	21	23743.462	4	23736.395	5			24614.255	-2		
9	22629.754	-22	22621.038	11	22613.073	2	23751.468	1	23742.720	1	23734.765	2			24613.473	3		
10	22629.893	19	22620.257	1			23751.510	-5	23741.904	7	23733.057	5	24622.152	-4	24612.588	-8		
11			22619.407	-2	22609.649	-26	23751.480	1	23740.994	1	23731.269	10	24622.074	17	24611.627	-5		
12	22629.838	2	22618.491	8			23751.355	-5	23740.006	-0	23729.395	12	24621.876	7				
13	22629.691	-9	22617.476	-5			23751.155	-1	23738.943	6	23727.426	3	24621.600	8	24609.446	1	24595.889	-1
14	22629.468	-18	22616.399	-3	22604.007	12	23750.863	-7	23737.789	2	23725.385	6	24621.218	-9	24608.208	-11	24593.689	-0
15			22615.239	-6	22601.949	3	23750.493	-8	23736.546	-7	23723.265	12			24606.904	-2	24593.689	-0
16	22628.816	-6	22614.007	-4	22599.832	14	23750.041	-7	23735.236	-2	23721.040	-4	24620.240	11			24591.398	-3
17			22612.706	6	22597.602	-11	23749.507	-4	23733.836	-3	23718.757	5	24619.614	17			24589.041	18
18	22627.841	-3	22611.316	4	22595.322	-7	23748.889	-2	23732.355	-3	23716.381	5	24618.884	8	24602.430	-6	24586.553	-5
19			22609.834	-11	22592.982	15	23748.181	-6	23730.796	1	23713.924	7	24618.063	-2	24600.756	-15		
20	22626.553	-0	22608.291	-11			23747.399	-1	23729.148	-1			24617.167	1	24599.018	2	24581.361	3
21	22625.800	11	22606.682	2			23746.531	2	23727.426	6	23708.767	19	24616.181	5			24578.652	26
22	22624.953	7	22604.975	-7	22585.414	2	23745.590	17	23725.606	-3	23706.038	-2			24595.242	0		
23	22624.025	-0	22603.223	17	22582.755	18	23744.536	1	23723.716	1	23703.239	-8	24613.925	-5	24593.228	5	24572.890	-4
24	22623.037	11	22601.359	7	22579.995	11	23743.411	-1	23721.739	1	23700.384	14	24612.678	6	24591.098	-16	24569.886	-9
25	22621.942	-5	22599.418	-3			23742.199	-6	23719.676	-3	23697.414	3	24611.325	2	24588.906	-11	24566.792	-13
26	22620.790	1	22597.416	4			23740.912	-2	23717.537	-0	23694.375	7	24609.879	-8	24586.625	-6	24563.624	-4
27	22619.550	-3	22595.322	-3			23739.530	-10					24608.370	11	24584.264	9		
28	22618.242	5	22593.156	-4	22568.192	4	23738.081	0	23713.004	0	23688.044	12	24606.753	11	24581.791	0	24556.991	-12
29	22616.822	-21	22590.925	8	22565.033	-9	23736.546	9	23710.615	3			24605.043	9	24579.242	5	24553.553	-3
30	22615.363	-5	22588.592	-4	22561.818	-1	23734.905	-4	23708.137	-1	23681.377	17	24603.241	5	24576.579	-15	24550.024	4
31	22613.815	-0	22586.189	-9	22558.517	2	23733.194	-3	23705.581	1			24601.353	6	24573.855	-5		
32	22612.191	7	22583.715	-6			23731.398	-3	23702.942	3	23674.364	11			24571.044	6	24542.682	4
33	22610.464	-8	22581.164	-3			23729.511	-9	23700.211	-5	23670.731	7					24538.874	2
34	22608.692	11	22578.543	10	22548.131	-5	23727.538	4	23697.414	7	23666.991	-19	24595.142	7	24565.127	5	24535.009	33
35			22575.820	-2	22544.512	-6	23725.497	-8	23694.519	3			24592.896	13	24562.032	3	24530.995	6
36	22604.872	12	22573.024	-8	22540.823	1	23723.364	-6			23659.341	9	24590.555	16	24558.849	3	24526.920	8
37	22602.820	-10	22570.170	6			23721.145	-4	23688.488	5			24588.088	-16	24555.572	1	24522.752	7
38	22600.734	13	22567.216	-1	22533.220	28	23718.837	-8	23685.354	12	23651.315	-2	24585.564	-12	24552.209	3	24518.489	3
39	22598.549	18	22564.185	-7	22529.241	-18	23716.447	-8	23682.121	4			24582.959	2	24548.752	2	24514.126	-11
40	22596.270	8	22561.084	-5	22525.248	0	23713.985	5	23678.818	11	23642.953	-12	24580.247	1	24545.201	-2	24509.693	-3
41	22593.906	-7					23711.406	-14	23675.424	11	23638.650	-12			24541.567	3	24505.160	-5
42	22591.487	4	22554.646	1	22517.013	28			23671.946	11	23634.259	-17	24574.526	-21	24537.833	-1	24500.549	7
43	22588.981	7	22551.313	9	22512.729	-6			23668.369	-5	23629.800	-4	24571.554	-5	24534.014	3	24495.823	-4
44	22586.394	10	22547.882	4	22508.446	41			23664.729	1					24530.097	-0	24491.018	-3
45	22583.715	1	22544.390	-3	22503.991	-6	23700.330	5	23660.998	1	23620.604	-3	24565.309	8	24526.093	2	24486.129	7
46	22580.963	-1	22540.823	13			23697.336	-1	23657.187	4	23615.864	-18	24562.032	-1	24521.991	-1		
47			22537.180	28	22494.926	-15	23694.270	7	23653.296	13	23611.061	-10	24558.660	-11	24517.801	2	24476.045	-3
48			22533.400	-16	22490.299	5	23691.112	8					24555.215	0	24513.517	3	24470.872	-0

TABLE 1—Continued

J	0-1 BAND				0-0 BAND				1-0 BAND									
	R(J)	O-C	Q(J)	O-C	P(J)	O-C	R(J)	O-C	Q(J)	O-C	P(J)	O-C	R(J)	O-C	Q(J)	O-C	P(J)	O-C
49	22572.230	2	22529.591	-10			23687.861	2	23645.205	-26	23601.186	-10	24551.661	-3	24509.145	10	24465.590	-14
50	22569.152	-3	22525.698	-8	22480.771	11	23684.510	-16	23641.058	-19			24548.010	-10	24504.663	-1	24460.231	-11
51			22521.740	8	22475.884	10	23681.123	15			23590.994	13	24544.279	-1	24500.092	-5		
52	22562.761	-4	22517.676	-1			23677.605	2			23585.752	7	24540.435	-11	24495.436	-1		
53	22559.462	13					23674.010	-2	23628.084	-23	23580.395	-29	24536.508	-8	24490.681	-1		
54	22556.060	9	22509.325	-4			23670.334	-1			23574.996	-22	24532.509	19	24485.847	15	24437.854	-6
55	22552.562	-10	22505.047	11					23619.006	-28	23569.531	6	24528.364	-5			24432.029	-0
56	22549.017	5	22500.681	20					23614.353	-15	23563.934	-15	24524.128	-23			24426.107	3
57	22545.379	9	22496.193	-15			23658.782	2			23558.281	-5	24519.837	0	24470.714	4	24420.098	14
58	22541.632	-13	22491.666	-7			23654.759	4	23604.777	-5			24515.441	15	24465.477	-1	24413.972	3
59	22537.826	-14	22487.050	-8			23650.644	2			23546.698	-3	24510.941	23	24460.147	-1	24407.763	4
60			22482.352	-11			23646.444	2	23594.838	-13			24506.332	19	24454.721	-0	24401.442	-11
61			22477.596	10			23642.149	-5	23589.781	23	23534.768	-6	24501.604	-6	24449.196	-1	24395.051	1
62	22525.937	6	22472.722	-8			23637.764	-15	23584.588	11			24496.806	-2			24388.536	-16
63			22467.787	-6			23633.316	1	23579.302	-9	23522.507	5	24491.910	2	24437.854	-1	24381.953	-4
64			22462.779	5			23628.766	2	23573.963	6	23516.231	-4	24486.917	7	24432.029	-6	24375.272	7
65			22457.684	10			23624.109	-15	23568.509	-7	23509.890	7	24481.810	-2	24426.107	-9	24368.483	7
66	22508.902	1	22452.495	1			23619.417	20	23562.984	-6	23503.447	3	24476.622	7	24420.098	1	24361.595	5
67	22504.432	-4					23614.587	7			23496.902	-17	24471.322	4	24413.972	-6	24354.622	16
68									23551.682	7	23490.297	-9			24407.763	4	24347.530	5
69	22495.254	-6					23604.692	10	23545.893	7	23483.605	-2	24460.434	11	24401.442	5	24340.337	-8
70	22490.540	-6							23540.029	17			24454.829	4	24394.995	-18	24333.059	-8
71	22485.761	11							23534.056	7					24388.463	-23		
72							23589.150	-18	23527.988	-9					24381.862	5		
73									23521.880	20					24375.117	-5		
74							23578.372	-7	23515.663	29			24431.412	-7	24368.282	-1		
75									23509.346	27					24361.339	1		
76							23567.227	-3	23502.918	2					24354.284	-4		
77							23561.505	-17	23496.429	4			24412.799	8	24347.136	7		
78													24406.370	-6	24339.850	-12		
79													24399.830	-26				
80													24393.229	-4	24324.992	-11		
81															24317.407	1		
82															24309.708	10		
83															24301.884	6		
84																		
85															24285.896	2		
86															24277.752	24		
87															24269.457	12		
88																		
89															24252.531	12		
90															24243.869	-6		
91															24235.100	-8		
92															24226.214	-3		
93															24217.196	-2		

TABLE II

Observed Wavenumbers (in  $\text{cm}^{-1}$ ) of the 0-1, 0-0, and 1-0 Bands of the  $[23.8]1-X0^+$  System of  $^{187}\text{ReN}$ 

J	0-1 BAND					0-0 BAND					1-0 BAND							
	R(J)	O-C	Q(J)	O-C	P(J)	O-C	R(J)	O-C	Q(J)	O-C	P(J)	O-C	R(J)	O-C	Q(J)	O-C	P(J)	O-C
3									23745.926	1								
4									23745.590	-6					24616.181	-20		
5	22628.993	-12	22623.752	8					23745.185	-1					24615.762	-2		
6	22629.397	-18	22623.295	13	22617.990	2	23750.816	-10	23744.687	-5			24621.329	-8	24615.230	-9		
7	22629.743	-5	22622.744	1	22616.563	0	23751.116	-7	23744.125	8	23737.921	-17	24621.597	4	24614.616	-11		
8	22629.996	-7	22622.126	-0	22615.051	-10	23751.357	21	23743.462	2	23736.395	1			24613.925	-3	24606.905	-0
9			22621.434	1	22613.506	26	23751.468	1	23742.720	-0	23734.765	-2	24621.839	0	24613.129	-12	24605.243	6
10	22630.296	17	22620.654	-9	22611.824	2	23751.510	-4	23741.904	6	23733.057	1	24621.839	10			24603.477	-3
11			22619.816	1			23751.480	2	23740.994	0	23731.269	6	24621.745	15	24611.306	2	24601.636	1
12			22618.892	2	22608.291	20	23751.355	-3	23740.006	-1	23729.395	8	24621.542	-0	24610.243	-11	24599.696	-5
13	22630.090	-16	22617.894	6	22606.381	2	23751.155	1	23738.943	5	23727.426	-2	24621.262	-4	24609.107	-10		
14	22629.893	1	22616.822	12	22604.414	5	23750.863	-5	23737.789	2	23725.385	0	24620.895	-7	24607.887	-5	24595.558	-12
15	22629.602	3	22615.653	-1	22602.368	8	23750.493	-5	23736.546	-7	23723.265	6	24620.422	-25	24606.576	-2	24593.387	16
16	22629.222	-6	22614.427	7	22600.219	-15	23750.041	-3	23735.236	-1	23721.040	-10	24619.893	-12	24605.187	9	24591.098	14
17	22628.766	-12	22613.121	11	22598.026	-4	23749.507	0	23733.836	-2	23718.757	-1	24619.271	-2	24603.685	-3	24588.712	4
18	22628.261	10	22611.726	5	22595.748	0	23748.889	2	23732.355	-2	23716.381	-2	24618.553	0	24602.115	3	24586.233	-11
19	22627.650	5	22610.257	0	22593.392	5	23748.181	-1	23730.796	2	23713.924	-1	24617.742	-1	24600.448	1	24583.698	7
20	22626.942	-18	22608.715	1	22590.925	-24	23747.399	5	23729.148	0	23711.389	6	24616.844	1	24598.703	10	24581.058	10
21	22626.210	13	22607.092	-1	22588.451	19	23746.531	8	23727.426	7	23708.767	9	24615.848	-7	24596.859	7	24578.319	1
22	22625.358	3	22605.397	2	22585.826	-12			23725.606	-2	23706.042	-8	24614.772	-4	24594.923	1	24575.499	1
23	22624.425	-10	22603.624	3	22583.168	3	23744.536	8	23723.716	2	23703.249	-9	24613.612	3	24592.899	-4	24572.600	10
24	22623.420	-15	22601.771	3	22580.417	4	23743.411	6	23721.739	2	23700.384	1			24590.798	3	24569.597	5
25	22622.346	-11	22599.832	-6			23742.199	2	23719.676	-2	23697.414	-10	24611.001	-3	24588.602	2	24566.499	-6
26	22621.191	-9	22597.832	2			23740.912	6	23717.537	1	23694.375	-8	24609.556	-11	24586.318	3	24563.332	2
27	22619.957	-7	22595.748	3	22571.679	-11	23739.530	-1					24608.033	-7	24583.952	10	24560.064	-0
28	22618.631	-19	22593.576	-5	22568.635	9	23738.081	10	23713.004	1	23688.044	-5	24606.423	0	24581.490	11	24556.708	-2
29	22617.256	1	22591.347	8	22565.500	17	23736.546	18	23710.615	3	23684.759	2	24604.712	-4	24578.933	7	24553.271	5
30	22615.784	1	22589.018	-3			23734.905	5	23708.137	-2	23681.377	-4	24602.916	-2	24576.297	11	24549.745	13
31	22614.230	-0	22586.630	6	22558.978	14	23733.194	6	23705.581	-0			24601.019	-10	24573.566	11	24546.119	11
32	22612.589	-10	22584.150	1	22555.594	8	23731.398	6	23702.942	1	23674.373	-4	24599.039	-12	24570.741	7	24542.400	5
33			22581.600	4	22552.129	-0	23729.511	0	23700.211	-8	23670.740	-10	24596.980	-1			24538.597	5
34	22609.095	-4	22578.965	0	22548.603	10	23727.558	13	23697.414	3	23667.037	-3	24594.819	-0	24564.828	5	24534.699	0
35	22607.233	3	22576.259	3	22544.975	-4	23725.497	1	23694.519	-3	23663.236	-9	24592.562	-6	24561.737	4	24530.719	4
36	22605.259	-22	22573.472	3	22541.277	-10	23723.364	3			23659.365	-2	24590.236	12	24558.553	1	24526.645	4
37	22603.223	-29	22570.598	-5	22537.521	5	23721.145	4	23688.488	-3	23655.399	-5	24587.789	0	24555.289	9	24522.476	0
38	22601.141	-3	22567.661	2	22533.660	-5	23718.837	0	23685.354	3	23651.357	-1	24585.254	-9	24551.922	3	24518.231	10
39	22598.961	5	22564.638	2	22529.736	-0	23716.447	-0	23682.121	-7			24582.649	4	24548.469	4	24513.875	0
40	22596.674	-15	22561.531	-4	22525.698	-29	23713.985	11	23678.818	-2	23643.021	9	24579.933	-1	24544.919	-2	24509.448	10
41	22594.341	-0	22558.356	1	22521.638	-2	23711.421	7	23675.424	-5	23638.715	2	24577.134	2	24541.283	-3	24504.907	-3
42	22591.915	1	22555.091	-5	22517.468	-5	23708.767	-3	23671.946	-6	23634.327	-3	24574.235	-1	24537.559	0	24500.296	6
43	22589.406	0	22551.764	5			23706.024	-17	23668.388	-5	23629.872	9	24571.258	8	24533.736	-3	24495.582	2
44	22586.830	12	22548.342	-1	22508.902	-2	23703.229	3	23664.749	-1					24529.830	1	24490.771	-6
45	22584.150	0	22544.842	-6	22504.491	-8	23700.330	5	23661.024	1	23620.676	2	24565.002	7	24525.823	-2		
46	22581.395	-7	22541.277	4	22500.049	34	23697.336	-3	23657.804	-7	23615.963	11	24561.737	8	24521.729	-0	24480.893	-3
47	22578.556	-16	22537.619	-1	22495.480	28	23694.270	3	23653.314	-1	23611.151	4	24558.363	-5	24517.536	-4		
48	22575.663	0	22533.896	9	22490.833	23	23691.112	2					24554.918	4	24513.250	-9		

TABLE II—Continued

J	0-1 BAND						0-0 BAND						1-0 BAND					
	R(J)	O-C	Q(J)	O-C	P(J)	O-C	R(J)	O-C	Q(J)	O-C	P(J)	O-C	R(J)	O-C	Q(J)	O-C	P(J)	O-C
49	22572.669	-4	22530.077	3	22486.062	-5	23687.861	-6	23645.280	11	23601.292	11	24551.362	-4	24508.881	-3	24465.384	2
50	22569.595	-7	22526.192	9	22481.273	-11			23641.132	13			24547.724	0	24504.408	-7	24460.023	-1
51	22566.460	10			22476.392	-10	23681.123	1			23591.078	3	24543.982	-5	24499.849	-3	24454.558	-16
52	22563.217	1	22518.142	-19	22471.415	-25	23677.622	2			23585.846	2	24540.159	4	24495.191	-4		
53	22559.911	8			22466.391	-7	23674.033	0	23628.153	-8	23580.535	6	24536.233	4	24490.441	-3		
54	22556.517	10	22509.802	-18	22461.257	-19	23670.356	-3			23575.123	-4	24532.206	-0	24485.591	-6	24437.647	-14
55	22553.037	6	22505.524	-5	22456.047	-27	23666.594	-4	23619.097	1	23569.636	-5	24528.080	-9	24480.650	-5	24431.830	-6
56	22549.468	-5	22501.153	-5	22450.761	-30	23662.740	-10	23614.435	-1	23564.076	7	24523.880	5	24475.609	-9	24425.916	0
57	22545.841	8	22496.708	1			23658.806	-11			23558.415	4	24519.568	3	24470.475	-10	24419.894	-7
58	22542.099	-12	22492.168	-8			23654.791	-5	23604.858	-2	23552.661	-6	24515.152	-7	24465.251	-4	24413.787	-5
59			22487.561	-4			23650.682	-5			23546.839	1	24510.660	4	24459.922	-6		
60	22534.437	14	22482.870	-1			23646.494	2	23594.940	-1	23540.906	-16	24506.052	-3	24454.502	-2	24401.275	-10
61	22530.456	-0	22478.103	4			23642.205	-4	23589.850	-2	23534.909	-11	24501.347	-11	24448.971	-12	24394.884	-5
62	22526.419	12	22473.242	-2			23637.837	-3	23584.688	11	23528.825	-7	24496.564	3			24388.378	-17
63	22522.270	-4	22468.302	-6			23633.378	-3	23579.423	8	23522.639	-19	24491.675	7	24437.647	2	24381.799	-7
64	22518.062	1	22463.295	3			23628.831	-5	23574.071	2	23516.389	-7	24486.687	12	24431.830	2	24375.117	-2
65			22458.188	-6			23624.212	9	23568.638	4	23510.055	6			24425.916	3	24368.332	-3
66			22453.012	-3			23619.487	5	23563.119	5	23503.616	1	24476.408	15	24419.894	-3	24361.460	7
67	22504.930	9					23614.662	-10	23557.505	-1	23497.092	-1	24471.111	9	24413.787	6	24354.476	2
68									23551.814	3	23490.482	-3	24465.716	5	24407.572	8	24347.393	-3
69	22495.731	-16					23604.777	-11	23546.030	1	23483.775	-15	24460.231	12	24401.233	-13	24340.215	-4
70	22491.047	13									23477.001	-5	24454.616	-11	24394.829	4	24332.972	29
71	22486.241	3					23594.546	-3	23534.213	10					24388.313	10	24325.580	13
72	22481.353	-6					23589.314	17	23528.157	-2	23463.186	9			24381.685	7	24318.114	23
73							23583.951	-4	23522.025	-1	23456.139	8	24437.258	19	24374.964	15	24310.534	19
74	22471.341	-7					23578.528	5	23515.806	0	23449.026	28			24368.127	11	24302.864	26
75	22466.251	35					23573.005	3	23509.487	-11	23441.783	8	24425.146	12	24361.197	18		
76							23567.383	-9	23503.103	3			24418.930	3	24354.157	21		
77							23561.716	24					24412.624	10	24346.992	6		
78									23490.042	2			24406.194	-4	24339.741	11		
79									23483.379	3			24399.673	-2				
80							23544.055	6	23476.626	3			24393.052	5	24324.896	-1		
81							23537.987	-1	23469.790	9			24386.313	1	24317.310	-7		
82							23531.848	13	23462.836	-13			24379.469	-2	24309.605	-23		
83															24301.813	-15		
84									23448.710	-6			24365.458	-7	24293.881	-37		
85									23441.499	-15			24358.303	4				

\*Observed minus calculated line positions (in units of  $10^{-3} \text{ cm}^{-1}$ ) using the constants of Tables III and IV.



TABLE III  
Rotational Constants (in  $\text{cm}^{-1}$ ) Obtained for the  $X0^+$  State  
of  $^{185}\text{ReN}$  and  $^{187}\text{ReN}$

Constants	$^{185}\text{ReN}$		$^{187}\text{ReN}$	
	v=0	v=1	v=0	v=1
$T_v$	0.0	1121.9216(19)	0.0	1121.5192(15)
$B_v$	0.481207(19)	0.478651(19)	0.4811223(88)	0.4785388(93)
$10^7 \times D_v$	2.877(75)	2.910(77)	4.019(14)	4.005(20)
$10^{12} \times H_v$	-7.59(88)	-8.28(92)	4.907(67)	4.62(19)

Note. The numbers in parentheses are one standard deviation in the last digit.

Each line was given an appropriate weight depending on the signal-to-noise ratio and the extent of blending. In the beginning, each band was fitted separately but in the final fit all three bands for each isotopomer were fitted together. The spectroscopic constants for the  $X0^+$  state of both isotopomers are reported in Table III, while the constants for the excited state are reported in Table IV. We have chosen to label the excited state as [23.8]1 with the origin of the state (in units of  $10^3 \text{ cm}^{-1}$ ) in square brackets followed by the  $\Omega$  assignment (26).

The rotational constants reported in Tables III and IV have been used to determine the equilibrium molecular constants in the ground and excited states for both isotopomers. The equilibrium constants for  $^{185}\text{ReN}$  are provided in Table V and those for

TABLE IV  
Rotational Constants (in  $\text{cm}^{-1}$ ) Obtained for the [23.8]1 State  
of  $^{185}\text{ReN}$  and  $^{187}\text{ReN}$

Constants	$^{185}\text{ReN}$		$^{187}\text{ReN}$	
	v=0	v=1	v=0	v=1
$T_v$	23746.4159(11)	24617.4042(14)	23746.4185(9)	24617.0742(10)
$B_v$	0.439895(18)	0.437273(19)	0.4397988(90)	0.4372113(88)
$10^7 \times D_v$	3.782(73)	4.593(73)	4.783(16)	5.695(13)
$10^{11} \times H_v$	-0.728(85)	-1.201(84)	0.4016(90)	--
$10^4 \times q_v$	-4.797(11)	-4.744(34)	-4.7244(75)	-4.442(20)
$10^4 \times q_{Dv}$	0.635(28)	5.51(25)	0.490(17)	1.962(94)
$10^{12} \times q_{Hv}$	--	-9.39(56)	--	2.13(10)
$10^{15} \times q_{Lv}$	--	1.085(41)	--	--

Note. The numbers in parentheses are one standard deviation in the last digit.

TABLE V  
Equilibrium Constants (in  $\text{cm}^{-1}$ ) for the  $X0^+$  and  
[23.8]1 States of  $^{185}\text{ReN}$

Constants	[23.8]1	$X0^+$
$B_e$	0.441206(22)	0.482485(24)
$\alpha_e$	0.002622(26)	0.002556(27)
$r_e(\text{\AA})$	1.71322(4)	1.63830(4)
$\Delta G(1/2)$	870.9883(18)	1121.9216(19)

Note. The numbers in parentheses are one standard deviation in the last digit.

$^{187}\text{ReN}$  are in Table VI. The equilibrium constants have been used to test the consistency of the isotopic relationships (27),  $B_e^i = \rho^2 B_e$ ,  $\omega_e^i = \rho \omega_e$ , and  $\alpha_e = \rho^3 \alpha$ , where  $\rho = (\mu/\mu^i)^{1/2}$ . Since the vibrational frequency  $\omega_e$  in the involved states could not be determined experimentally because no bands with  $v > 1$  were observed, we have used the  $\Delta G(1/2)$  values instead of  $\omega_e$  in the isotopic relations. The values for the ground state of the minor isotopomer  $^{185}\text{ReN}$  calculated from  $^{187}\text{ReN}$  are  $B_e = 0.48277$ ,  $\Delta G(1/2) = 1121.9423$ , and  $\alpha_e = 0.00259 \text{ cm}^{-1}$ , in moderate agreement with the observed values of  $B_e = 0.482485$ ,  $\Delta G(1/2) = 1121.9216$ , and  $\alpha_e = 0.002556 \text{ cm}^{-1}$ . The corresponding calculated values for the excited state of  $^{185}\text{ReN}$  are  $B_e = 0.44143$ ,  $\Delta G(1/2) = 870.9842$ , and  $\alpha_e = 0.00259 \text{ cm}^{-1}$ . These are also in reasonable agreement with the observed excited state values, which are  $B_e = 0.441206$ ,  $\Delta G(1/2) = 870.9883$ , and  $\alpha_e = 0.002622 \text{ cm}^{-1}$ .

The equilibrium rotational constants obtained were used to evaluate the equilibrium bond lengths in the ground and excited states of ReN (Tables V and VI). The observed ground state bond length of  $1.63780(2) \text{ \AA}$  is slightly smaller than the ground state bond length of ReO ( $r_e'' = 1.6404 \text{ \AA}$ ).

TABLE VI  
Equilibrium Constants (in  $\text{cm}^{-1}$ ) for the  $X0^+$  and  
[23.8]1 States of  $^{187}\text{ReN}$

Constants	[23.8]1	$X0^+$
$B_e$	0.441093(11)	0.482414(11)
$\alpha_e$	0.002588(13)	0.002584(13)
$r_e(\text{\AA})$	1.71280(3)	1.63780(2)
$\Delta G(1/2)$	870.6557(14)	1121.5192(15)

Note. The numbers in parentheses are one standard deviation in the last digit.

(b) *Laser Excitation Spectroscopy*

Although the Fourier transform measurements provided a set of precise spectroscopic constants, there are some potential problems with the analysis. Since the Fourier transform spectra were recorded in emission, there is no proof that the lower state of the observed transition is the ground state. In addition, first lines were not detected so that the  $\Omega$  quantum numbers of the two states could not be definitively assigned and the possibility of a  $[23.8]0^+ - X1$  rather than  $[23.8]1 - X0^+$  transition could not be excluded. The laser excitation spectra recorded at the University of Victoria provided complementary information and confirmed the assignment.

The laser excitation spectrum (Fig. 3) of the  $[23.8]1 - X0^+$  transition of the cold ReN molecule showed clearly the first *R* line ( $R(0)$ ) and also the first *Q* line ( $Q(1)$ ). This confirmed the  $\Omega$  assignments for the two electronic states, although the  $X0^+$  and  $X0^-$  assignments still cannot be distinguished on the basis of the experimental data alone. The lower state of the  $[23.8]1 - X0^+$  transition is almost certainly the ground state since the laser excites molecules from the same lower state that is seen in the emission spectrum. Within experimental error, the line positions and the spectroscopic constants derived from the laser experiments are the same as those from the emission work (but of lower precision). It should be noted that the possibility that the lower state of the transition is a low-lying metastable state can not be completely excluded. The use of a pulsed laser also allowed the radiative lifetime of the  $[23.8]1$  state of ReN to be determined. A single exponential decay of the excited state fluorescence was found with a lifetime of  $201 \pm 1$  nsec. Research is continuing on the electronic spectrum of ReN at the University of Victoria.

DISCUSSION

The electronic spectrum of ReN is expected to be very similar to the spectrum of the isoelectronic molecule WO. The spectrum of WO has been studied by Samoilova *et al.* (28) who observed several  $\Delta\Omega = 0$  and  $\Delta\Omega = 1$  electronic transitions in the

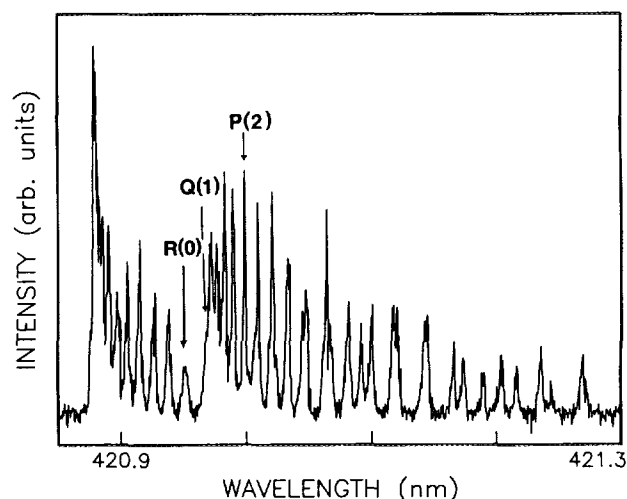


FIG. 3. The laser excitation spectrum of the 0-0 band of the  $[23.8]1 - X0^+$  system of ReN near the band origin showing the first *R*, *Q*, and *P* lines.

visible region involving the  $X0^+$  state. Samoilova *et al.* (28) concluded that the ground state is most probably a  $0^+$  component of a case (c)  $X^3\Sigma^-$  state with a configuration of  $\delta^2\sigma^2$ . There are no theoretical calculations or other evidence to support this conclusion.

In contrast to WO, the other group VIB oxides, CrO (29) and MoO (30), are known to have  $X^5\Pi$  ground states. Although it seems very unlikely, we can not rule out an  $X^5\Pi$  ground state for ReN on the basis of the available experimental data. In Hund's case (c) coupling, the bands due to the different spin components,  $^5\Pi_3$ ,  $^5\Pi_2$ ,  $^5\Pi_1$ ,  $^5\Pi_0$ ,  $^5\Pi_{-1}$ , could be far apart with  $^5\Pi_{0+}$  as the lowest energy spin component. Similarly a  $^7\Sigma^+$  state or a  $^5\Sigma^+$  state, which are calculated as the lowest energy states in ReH (31), are also possible ground states for ReN since these two terms provide  $0^-$  states in Hund's case (c) coupling. In this case, the unassigned weak bands could be due to the other spin components. Some *ab initio* calculations on ReN would be very welcome!

#### CONCLUSION

We have observed the emission spectrum of the [23.8]1- $X0^+$  transition of ReN molecule by Fourier transform spectroscopy and laser excitation spectroscopy. The rotational analysis of 0-1, 0-0, and 1-0 bands of both  $^{187}\text{ReN}$  and  $^{185}\text{ReN}$  provided equilibrium constants for the ground and excited states. The ground state equilibrium bond length of 1.63780(2) Å is slightly shorter than that of ReO (20, 21) (1.6404 Å). Some *ab initio* calculations would be helpful in order to determine what the parent  $^{2S+1}\Lambda$  term is for the ground  $X0$  ( $0^+$  or  $0^-$ ) state.

#### ACKNOWLEDGMENTS

We thank J. Wagner, C. Plymate, and P. Hartmann of the National Solar Observatory for assistance in obtaining the spectra. The National Solar Observatory is operated by the Association of Universities for Research in Astronomy, Inc., under contract with the National Science Foundation. The research described here was supported by funding from the Petroleum Research Fund administered by the American Chemical Society. Support was also provided by the Center of Excellence in Molecular and Interfacial Dynamics (CEMAID) and the Natural Sciences and Engineering Research Council of Canada. We are thankful to R. Engleman for lending us his rhenium hollow cathode. The rhenium foil was provided by Johnson Matthey Co.

RECEIVED: June 6, 1994

#### REFERENCES

1. M. GRUNZE, in "The Chemical Physics of Solid Surfaces and Heterogeneous Catalysis" (D. A. King and D. P. Woodruff, Eds.), Vol. 4, pp. 143-194, Elsevier, New York, 1982.
2. N. N. GREENWOOD AND A. EARNSHAW, "Chemistry of the Elements," Pergamon, Oxford, 1984.
3. J. C. HOWARD AND J. G. CONWAY, *J. Chem. Phys.* **43**, 3055-2057 (1965).
4. T. M. DUNN AND M. K. RAO, *Nature (London)* **222**, 266-267 (1969).
5. R. S. RAM AND P. F. BERNATH, *J. Chem. Phys.* **96**, 6344-6347 (1992).
6. R. S. RAM AND P. F. BERNATH, *J. Opt. Soc. Am.* **11B**, 225-230 (1994).
7. R. S. RAM AND P. F. BERNATH, *J. Mol. Spectrosc.* **165**, 97-106 (1994).
8. T. M. DUNN, L. K. HANSON, AND K. A. RUBINSON, *Can. J. Phys.* **48**, 1657-1663 (1970).
9. J. K. BATES, N. L. RANIRI, AND T. M. DUNN, *Can. J. Phys.* **54**, 915-916 (1976).
10. S. L. PETER AND T. M. DUNN, *J. Chem. Phys.* **90**, 5333-5336 (1989).
11. B. SIMARD, C. MASONI, AND P. A. HACKETT, *J. Mol. Spectrosc.* **136**, 44-55 (1989).
12. W. J. BALFOUR, A. J. MERER, H. NIKI, B. SIMARD, AND P. A. HACKETT, *J. Chem. Phys.* **99**, 3288-3303 (1993).

13. J. K. BATES AND T. M. DUNN, *Can. J. Phys.* **54**, 1216–1223 (1976).
14. J. K. BATES AND D. M. GRUEN, *J. Chem. Phys.* **70**, 4428–4429 (1979).
15. J. K. BATES AND D. M. GRUEN, *High Temp. Sci.* **10**, 27–43 (1978).
16. J. K. BATES AND D. M. GRUEN, *J. Mol. Spectrosc.* **78**, 284–297 (1979).
17. L. B. KNIGHT AND J. STEADMAN, *J. Chem. Phys.* **76**, 3378–3384 (1982).
18. D. W. GREEN, W. KORMFMACHER, AND D. M. GRUEN, *J. Chem. Phys.* **58**, 404–405 (1973).
19. K. A. GINGERICH, *J. Chem. Phys.* **49**, 19–24 (1968).
20. W. J. BALFOUR AND R. S. RAM, *J. Mol. Spectrosc.* **100**, 164–173 (1983).
21. W. J. BALFOUR AND R. S. RAM, *Can. J. Phys.* **62**, 1524–1537 (1984).
22. O. LAUNILA, A. M. JAMES, AND B. SIMARD, *J. Mol. Spectrosc.* **164**, 559–569 (1994).
23. B. A. PALMER AND R. ENGLEMAN, "Atlas of the Thorium Spectrum," Los Alamos National Laboratory, Los Alamos, NM, 1983. [unpublished]
24. T. G. DIETZ, M. A. DUNCAN, D. E. POWERS, AND R. E. SMALLEY, *J. Chem. Phys.* **74**, 6511–6512 (1981).
25. W. J. BALFOUR, J. CAO, C. X. W. QIAN, AND S. J. RIXON, unpublished.
26. C. LINTON, M. DULICK, R. W. FIELD, P. CARETTE, P. C. LEYLAND, AND R. F. BARROW, *J. Mol. Spectrosc.* **102**, 441–497 (1983).
27. G. HERZBERG, "Spectra of Diatomic Molecules," Van Nostrand, New York, 1950.
28. A. N. SAMOILOVA, Y. M. EFREMOV, AND L. V. GURVICH, *J. Mol. Spectrosc.* **86**, 1–15 (1981).
29. A. J. MERER, *Annu. Rev. Phys. Chem.* **40**, 407–438 (1988).
30. Y. M. HAMRICK, S. TAYLOR, AND M. D. MORSE, *J. Mol. Spectrosc.* **146**, 274–313 (1991).
31. D. DAI AND K. BALASUBRAMANIAN, *J. Mol. Spectrosc.* **158**, 455–467 (1993).